DOI: 10.13009/EUCASS2022-4583
9TH EUROPEAN CONFERENCE FOR AERONAUTICS AND SPACE SCIENCES (EUCASS)

Non-linear one-dimensional combustion response model integration in a CFD software, test case and simplified rocket motor applications

Maialen CARRICART[⋆], *Joël DUPAYS*[⋆] *and Jérôme ANTHOINE*[⋆]
[⋆]*DMPE, ONERA, Université Paris Saclay*
F-91123 Palaiseau-France
maialen.carricart@onera.fr · joel.dupays@onera.fr · jerome.anthoine@onera.fr

Abstract

The modelisation of propellant response function is a meaningful way to anticipate the growth of instabilities in some solid propellant motor combustion chambers. A non-linear, one-dimensional, quasi-steady and homogeneous model has been developed and introduced in CFD software to consider this effect in numerical simulations. The model has been tested throughout different simulations. First, with a simple test case to verify the numerical integration of the model into the software. Then with the simulation of a fictitious stable motor that has been destabilised and with a naturally unstable motor subject to a vortex shedding phenomenon. Finally, an experimental setup devoted to the characterisation of the propellant response function has been meshed and simulated. These simulations have shown the interest in taking into account the combustion response of propellant in the early studies of the motors to observe the level of instabilities in the combustion chambers.

1. Introduction

The civil and military rocket engines use solid propellant propulsion intensively. It allows significant thrust while being reliable and cheap. Solid propellants are energetic materials that reach a high temperature in the combustion chamber. Once the combustion is ignited, it is tough to stop it before consuming all the propellant. Then, it is essential to control the combustion process and anticipate the appearance of instabilities. The study of acoustics instabilities in combustion chambers is of primary concern in rocket motor development. However, if the instabilities were of hydrodynamic origin for the long EAP of Ariane 5, the combustion instabilities are more feared for smaller rocket engines. The coupling of those instabilities with the chamber acoustics can induce some strong thrust perturbations, possibly damaging for the mission. Each energy fluctuation, whatever the origin (turbulences, heterogeneity, . . .), can be amplified and coupled with the chamber acoustic resulting in injected mass flow and burnt gas temperature fluctuations; this coupling happens in a specific frequency range. For small engines, the combustion response of the propellant is the main source of instability.

In a solid propellant motor, the transformation of the energy stored in the molecular bonds into mechanical energy during combustion and the flow dynamics of the combustion products often play an active role in triggering instabilities. Recent experimental evidence on subscale motors suggests focusing on the possibility of a non-linear coupling between acoustics and propellant surface combustion. Based on the extensive work done before the 2000s at ONERA, the subject of the combustion response of solid propellant has been reinvested through the integration of a non-linear model [1] in the ONERA multi-physics CFD code CEDRE.

The combustion instabilities are mainly due to the difference in thermal inertia between the gas and the solid phases. The pressure changes in the gas phase induce an oscillation in thermal flux arriving on the combustion surface that implies mass flow rate oscillation. However, there is a phase and amplitude difference between the first pressure change and the resulting mass flow oscillation. This phenomenon is called the response of the propellant, and it is more critical in a specific frequency range. It is crucial to develop an unsteady combustion model, to anticipate this response. In the steady-state frame, it has been proven that the regression rate of a solid propellant depends mainly on the pressure according to an empirical law. It is the classical law used to describe steady-state combustion, but different

DOI: 10.13009/EUCASS2022-4583

models have been developed for unsteady situations.

The oldest response function models are the Quasi-steady Homogeneous One Dimensional (QSHOD). The problem of solid propellant combustion is addressed in one direction, only considering homogeneous propellants. Thus, the hypothesis is that the lateral phenomena in the propellant are negligible compared to the ones perpendicular to the surface. The gas phase is considered in a quasi-steady state, meaning that it responds instantaneously to chamber condition changes. There are two main families of QSHOD models, the ZN and FM models. The first one was developed in the soviet union by Zeldovich and Novozhilov [2, 3]. The other one is the flame model developed in the United States at the same time [4, 5]. These models are said to be "two-parameter" models because Culick in [6] showed that the two model families could express the response function depending on two parameters specific to the models.

From those models, many relaxations on the hypothesis have been studied to describe what is happening at the burning surface more precisely. Some studies concentrate on the dynamics of the gas phase [7, 8, 9, 10] which showed the appearance of a second response pic at higher frequencies. The heterogeneity of the most used propellant has also been studied, mostly to describe the composition and behaviour of the flame above the surface [11, 12, 13]. This description adds a lot of complexity to the model, and more reactions must be taken into account and modelled with often not enough physical properties information. Finally, non-linear pressure oscillations have also been studied [14, 15]. A simple way of considering large amplitude of pressure oscillation is to numerically integrate the equations, avoiding any linearisation.

However, any propellant description by mean of a model needs a precise propellant characterisation to pressure oscillations. The best way to do so is to use a dedicated experimental setup. Several experimental apparatus has been developed for this purpose. The most used one is the T-burner [16, 17], but we can also cite the modulated exhaust jet burner (MEJT) developed and used at ONERA [18, 19]. Numerical simulations of experimental apparatus allow confronting the numerical models to observed behaviours[20]. The presence of a non-linear model in the ONERA CFD code CEDRE and the available experimental data allow some simulation of the MEJT.

The model developed here is based on the work of Kuentzmann [1], a non-linear response model for homogeneous propellant. In the first part, the equations describing the combustion and the different phenomenon in the propellant are exposed. Then, the validation of the model in the linear frame is shown. A representative stable and unstable motor test cases are studied to assess our model, and then the simulation procedure of the MEJT apparatus is presented.

2. Response Model

The instabilities observed in a combustion chamber are induced by pressure oscillations. These oscillations disrupt the combustion of the solid propellant by oscillating the thermal flux arriving at the surface. Thus, due to the condensed phase's more significant thermal inertia compared to the burnt gases, some flow oscillations can appear at certain specific frequencies. The behaviour of the mass flow compared to the pressure in the burning surface is called the response of the solid propellant. This quantity is a transfer function between the two variables that can be expressed as:

$$R_{mp} = \frac{\dot{m}'/\overline{\dot{m}}}{P'/\overline{P}} \tag{1}$$

With $\dot{m}$ the mass flow rate and P the pressure.

In order to analyse this quantity, it is necessary to develop a model describing the combustion and the heat transfer at the burning surface and in the condensed phase. The model described here is a QSHOD family model, called KTZ, that is considering a quasi-steady gas phase based on the work of Kuentzmann [1]. The propellant is homogeneous with constant thermochemical properties. For heterogeneous propellants, it implies an averaging of the thermochemical properties that are not studied here.

The flame is described by a flame-sheet model. Figure 1 shows the coordinates and the physical problem taken into account. The equations are described separately in the different zone of interest.

DOI: 10.13009/EUCASS2022-4583

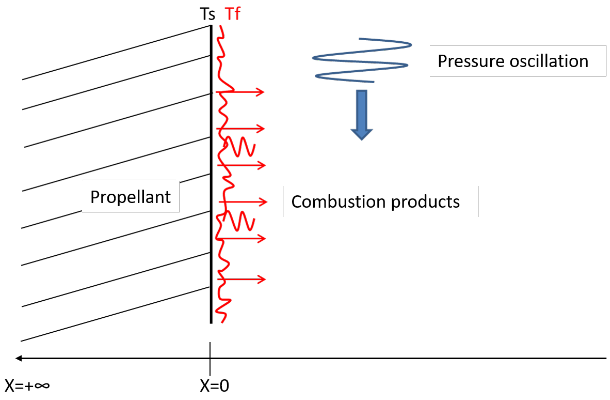

Figure 1: Scheme of response phenomena

2.1 Condensed phase (+∞ > x > 0)

The propellant in the solid phase is assumed to be inert and homogeneous with no chemical reactions. All the reactions are concentrated on the burning surface. The leading phenomenon in the solid is heat transfer. The energy equation in terms of temperature can be written as:

$$\frac{\partial}{\partial x^*}\left(\lambda\frac{\partial T}{\partial x^*}\right) = \rho C\frac{\partial T}{\partial t}, \tag{2}$$

With λ the propellant thermal conductivity, C the propellant heat capacity and ρ its density.

In our case, it is more convenient to change the reference frame to the burning surface. The instantaneous velocity of regression is then taken into account in the energy equation. The change of variable necessary to move the reference frame is the following:

$$x = x^* - \int_0^t v_b dt, \tag{3}$$

With v_b the regression rate. The equation 2 becomes:

$$\frac{\partial^2 T}{\partial x^2} + \frac{v_b}{a}\frac{\partial T}{\partial x} = \frac{1}{a}\frac{\partial T}{\partial t}, \tag{4}$$

With a the propellant thermal diffusivity.

Initial and boundary conditions are necessary to the numerical integration of the equation. At the beginning of the simulation, the temperature profile in the solid is initialised with the steady-state analytical profile. The propellant is considered semi-infinite, and thus the temperature in depth is fixed to be equal to the initial temperature of the propellant. The boundary condition at the propellant surface is the thermal flux coming from the flame that can be expressed:

$$q_S^+ = -\lambda\left(\frac{\partial T}{\partial x}\right)_{x=0}, \tag{5}$$

With q_S^+ the thermal flux arriving at the burning surface.

The propellant transforms into the gas phase through a pyrolysis process concentrated at the surface. The classical expression for pyrolysis is an Arrhenius relation between regression rate and surface temperature given by:

$$v_b = B_v exp\left(-\frac{E_S}{RuT_S}\right), \tag{6}$$

DOI: 10.13009/EUCASS2022-4583

With B_v the pyrolysis pre-exponential coefficient, E_s the pyrolysis reaction energy of activation and Ru the universal gas constant. However, at steady-state, the regression rate of a burning propellant surface follows the empirical Saint Robert and Vieille law. This law can be easily characterised in a laboratory for each propellant composition. It is given by:

$$\overline{v_b} = b\overline{P}^n exp\left(\sigma(T_i - T_R)\right), \tag{7}$$

With b and n the empirical Saint-Robert and Vieille coefficients, σ the temperature sensitivity coefficient and T_R the reference temperature. The integration of the steady-state energy equation gives the global thermal flux arriving at the surface used for the initialisation of the calculus.

$$\overline{q_S^+} = \rho C\overline{v_b}\left(\overline{T_S} - T_i\right), \tag{8}$$

The Kuentzmann approach to the problem is a ZN approach which stipulates that a functional relationship can be found to express the unsteady thermal flux arriving at the surface. In our case, the precedent steady-state expression is used for the unsteady expression replacing steady-state values of initial temperature and surface temperature with a functional relationship. Thus, giving an expression for the thermal flux:

$$q_S^+ = \rho C v_b\left(\frac{E_S}{Rln\frac{B_v}{v_b}} - T_R - \frac{1}{\sigma}ln\frac{v_b}{bP^n}\right), \tag{9}$$

For the numerical integration, it is necessary to connect with the gas phase and determine the flame temperature.

2.2 Gas phase ($-\infty$< x < 0)

The propellant combustion is described by a flame sheet model, which means that the flame is very thin and close to the propellant surface. Therefore, the combustion reaction can be described by an energy balance between the surface and the inert gas phase. The combustion reaction is a one-step reaction transforming propellant gases from pyrolysis to inert combustion gas products. The energy balance equation can be written as:

$$\rho_g v_g h_g(T_f) = \rho v_b h_p(T_S) - q_S^+, \tag{10}$$

With ρ_g, v_g and h_g the gas density, velocity and enthalpy respectively. The h_p is the propellant enthalpy and T_f the flame temperature.

The energy released during the combustion is defined as the difference between the enthalpies of formation of the solid propellant and the burnt gases. The steady-state flame temperature is defined easily with this quantity and depends on the composition of the reactants only. Thus, the unsteady flame temperature can be defined as a function of the reference one. It is then possible to rewrite the energy balance equation to express the flame temperature:

$$T_f = \overline{T_{fR}} + \frac{C}{C_p}\left(T_S - T_R - \frac{q_S^+}{\rho C v_b}\right) = \overline{T_{fR}} + \frac{C}{C_p}\left(\frac{1}{\sigma}ln\frac{v_b}{bP^n}\right) \tag{11}$$

With T_{fR} the flame reference temperature.

The combustion product gases are introduced into the chamber at the flame temperature. This model has been integrated into the laboratory CFD code as a boundary condition of a propellant surface. The energy equation is resolved using a Crank-Nicolson scheme, and the CFD code resolves the flow above the combustion surface with Navier-Stokes equations. This model is made with no linear assumption, thus allowing the simulation of large amplitude of pressure oscillations.

DOI: 10.13009/EUCASS2022-4583

3. Validation

The next step is to verify the behaviour of the model in the linear frame to ensure the good integration of the model in the CFD code. It is possible to express the response function in the classical two parameters equation by linearising the above equations. The pressure-coupled response function after linearizing is given in equation (12).

$$R_{MP} = \frac{nAB}{S + \frac{A}{S} - (1 + A) + AB} \tag{12}$$

$$S = \frac{1}{2} + \frac{1}{2}\sqrt{1 + 4i\Omega}, \Omega = \frac{2\pi f a}{v_b^2} \tag{13}$$

The link with our model is done with the definition of the coefficient A et B. They can be expressed as a function of the KTZ model properties: $A = ((1 - T_i/T_s)E_s)/(RT_s)$, $B = 1/(\sigma(T_s - T_i))$. In the simulation, the computation of the pressure-coupled response function is straightforward, given by the unsteady mass flow rate and pressure signal at the burning surface. The same response function must be found between the numerical model and the two-parameter expression when the pressure oscillations are in the linear frame. A one-cell mesh test case, shown in figure 2, is simulated to verify this behaviour.

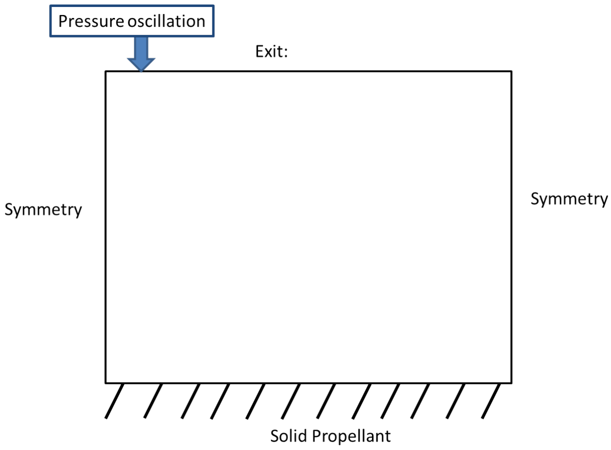

Figure 2: One-cell mesh test case

A small-amplitude sinusoidal pressure oscillation is introduced at the exit of the cell. The unsteady thermal flux arriving at the surface is computed, and the energy equation (4) numerically resolved. The surface temperature and regression rate are then deduced at the burning surface. Several frequencies are simulated, and the response function is computed to construct the classical response curve depending on the frequency.

The computation with the two-parameter response function is easy and does not depend on the amplitude of the introduced pressure signal but only on its frequency. For a pressure signal amplitude of 1% ($\Delta P/P$=1%), the comparison between the theoretical and simulated response function is plotted in figure 3. The two curves are in accordance even if a degradation at the high frequencies is observable for the numerical response due to the constant time step taken for every simulation showing that it is too big for high-frequency simulations. However, the model can be validated in the linear frame.

It was also interesting to observe the behaviour of our model in the non-linear frame, with bigger amplitudes of pressure oscillation. The figure 4 shows the response function obtained for an amplitude of 10% ($\Delta P/P$=10%). The response peak is shifted towards lower frequencies compared to the linear frame. The peak of the real part is greater, whereas the imaginary part is only shifted. At very low frequencies and higher frequencies, the behaviour of the non-linear simulation joins the linear one.

The one-cell case is straightforward to simulate and does not require many resources and time to test the response model to simple pressure oscillation. However, more realistic motor geometries must be tested to verify the importance of the response phenomenon on the combustion instabilities.

DOI: 10.13009/EUCASS2022-4583

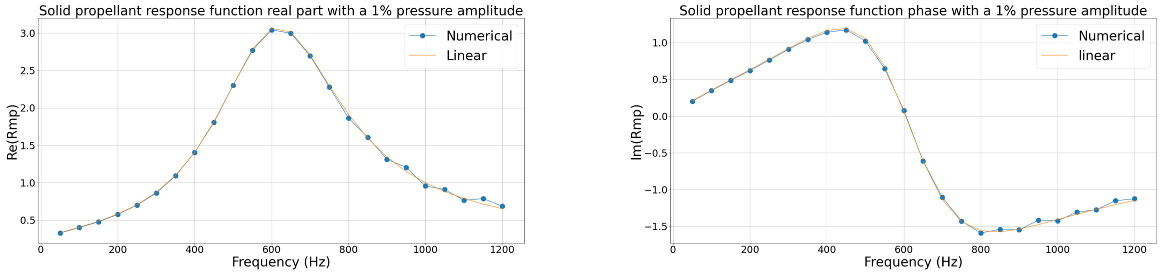

Figure 3: Response function comparison for a 1% pressure signal amplitude

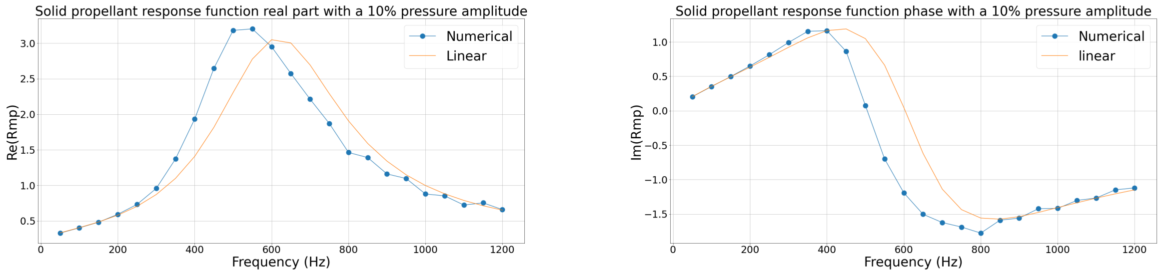

Figure 4: Response function comparison for a 10% pressure signal amplitude

4. TEP motor

The TEP motor is a naturally stable reference rocket motor studied for validation. It has a simple configuration representative of real solid-propellant rocket engines. Figure 5 represents the 2D axisymmetric geometry. The influence of the response on the propellant combustion can be observed with the numerical simulation of this motor using the KTZ model as a boundary condition. The study lead here is a verification of the behaviour of the response of the propellant to pressure oscillation in a rocket chamber. The purpose is to analyse the effect of solid propellant response on the pressure instability. The TEP motor being very stable, the instability must be imposed and the damping measured. This work has already been done for different linear response models by Vuillot at al. [21] with an impulsive method. The aim here is to compare the behaviour of the response modelled in the code with the response obtained in the paper.

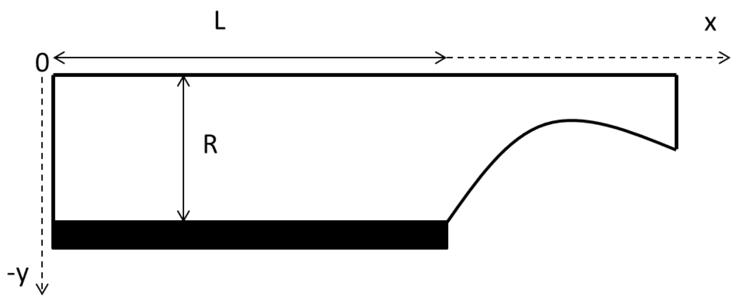

Figure 5: Scheme of TEP motor

In the article [21], the authors used an acoustic balance method to compute the contribution of the different elements of the motors on the acoustic. This linear stability method allows to estimate the damping or amplification effect of each element and thus, compute the global coefficient that is a sum of all these contributions. For example, the chamber walls and inert particles are known to attenuate acoustic instabilities, whereas combustion amplifies them. The acoustic balance allows comparing different combustion response model and their effect on the instabilities.

The simulation done here on the TEP motor is done in two-step. First, a Saint-Robert and Vieille law is used at the propellant surface to simulate the combustion, and the steady-state is reached. The motor is very stable; there

DOI: 10.13009/EUCASS2022-4583

are no instabilities inside the chamber. Then, the simulation is resumed, and a pressure oscillation is introduced at the chamber's front at 3162 Hz, which is the first chamber mode, during one period with a 1% amplitude. The acoustic damping of the chamber is deduced from the pressure signal at the front of the chamber that slowly recovers the steady-state pressure. The instability simulations are done with the KTZ model and Saint Robert and Vieille combustion law. Thus, the two combustion responses can be compared with the ones used in the reference [21]. The global damping coefficient for each simulation was computed through a non-linear regression on the pressure signal.

The response functions used in the reference [21] were generic two-parameter linear responses with a response peak at high frequencies. In order to compare the models, the propellant properties in our model were adapted to obtain the same linear response function (curve "f" from the reference with a peak around 2300Hz). The pressure signal at the front of the motor showing its stabilisation to the steady-state value with an AP^n law and with the response model is shown in the figure 6.

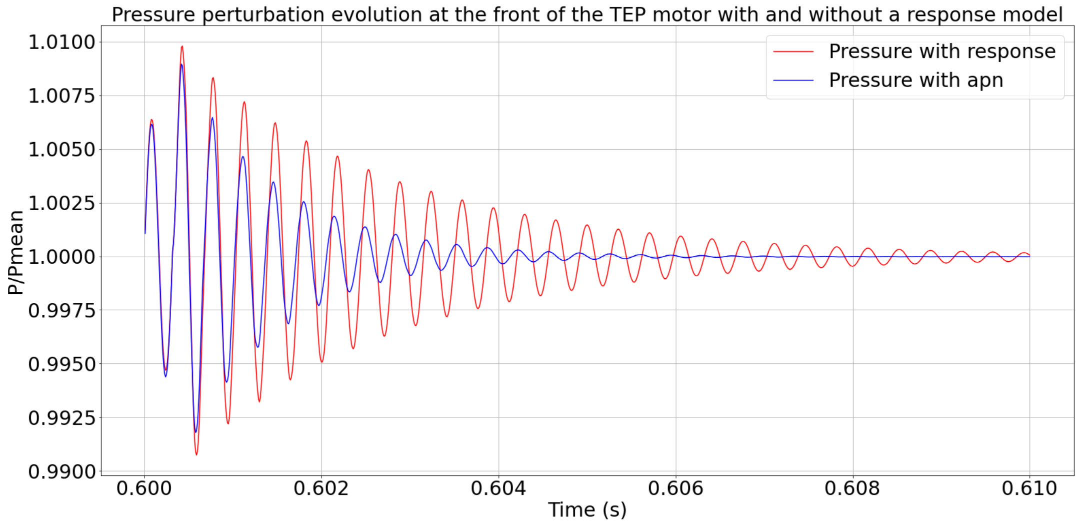

Figure 6: Pressure signal at the front of the motor

Applying a response model increases the amplitude of the introduced oscillations, and the time to recover a steady-state is therefore extended. Non-linear regression is done on the pressure signal peaks to compute the global damping coefficient. Then, the coefficients of the different models are compared to the theoretical value using an acoustic balance like in the reference [21]. To do so, the contribution of the combustion to the acoustic balance is computed with the equation (14).

$$\alpha_c = -\gamma \frac{V_{inj}}{R} Re(R_{mp}) \tag{14}$$

Different comparisons have been made in this test case, first, between an AP^n law and the KTZ model. Then, between the theoretical linear stability analysis and the simulations. The table 2 summarizes the results obtained for the response function and an AP^n law. The curve "f" on figure 7a is reproduced by playing on the linear response function parameters. The figure 7b shows the response function obtained that approximates the "f" curve.

The "Theoretical" coefficient is obtained by taking the acoustic balance coefficient without response function from the reference [21] and then by removing the combustion contribution obtained with the AP^n law and with our model, this coefficient being computed with the previous relation (14). The "numerical" coefficient is the one obtained with the regression on the numerical pressure signal. The influence of combustion on instabilities is shown by the difference between the coefficient obtained with a response model and an AP^n law. When there is a response function, the damping coefficient is less important than in the AP^n law case but the two values stays around the theoretical ones.

DOI: 10.13009/EUCASS2022-4583

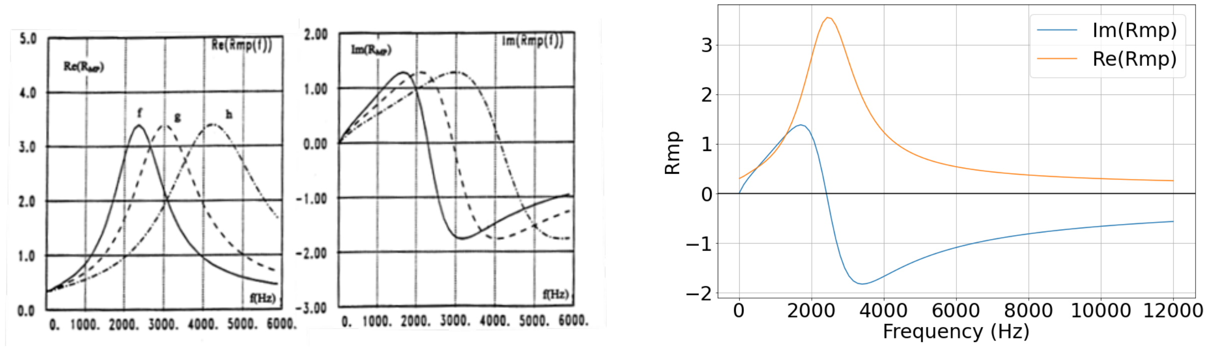

(a) Response curves of the article [21]

(b) Reproduction of the "f" curve

Figure 7: Response function as seen in the curve "f" of the reference [21]

	With Response		With AP^n	
	Theoretical	Numerical	Theoretical	Numerical
$\alpha\ (s^{-1})$	355.5	348.5	889	861

Table 1: Damping coefficient with different combustion models with a 1% pressure oscillation

The response function is then more destabilising than the steady state empirical AP^n law. The KTZ model is coherent with the theory showing the pertinence of the model in a real test case. It shows that our model reacts the same way as the predicted two parameter law.

The TEP motor being very stable the instability must be imposed but it is very intresting to look the effect of the response model on a naturally instable motor. This has been done through the C1x simulations.

5. C1x motor configuration

The C1x motor is a test motor designed to generate a vortex shedding phenomenon and spacially characterised thanks to the presence of a large number of sensors distributed along the same generatrice. It is a cylinder-type rocket motor with a cut propellant in the middle, allowing a step in the propellant grain. The C1x geometry is shown in figure 8 for the 2D axisymmetric simulation case. It was initially an experimental setup that has given a lot of data and information on the effect of this particular phenomenon. Since the early 90's, it has also been simulated thanks to CFD codes to identify the vortex shedding in the chamber and the effect of the instabilities on the motor performances [22, 23].

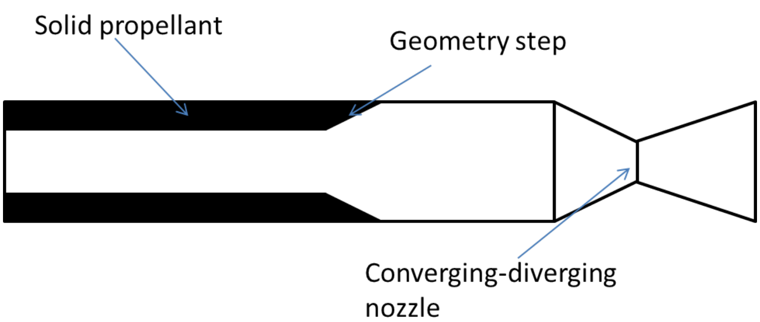

Figure 8: C1x motor scheme

The study here was meant to verify the effect of our response model on the natural instabilities in the C1x motor. A comparison with previous studies has been made by making the same simulation with several propellant boundary

DOI: 10.13009/EUCASS2022-4583

conditions. The first one was the fixed mass flow rate simulation given by a gas-flowing surface condition. The second simulation used a Saint-Robert and Vieille law to simulate the propellant gas flow in the chamber. These two simulations were injecting the burnt gases at the mean flame temperature. The last one is using the KTZ model, which computes the gas temperature depending on the instabilities in the chamber.

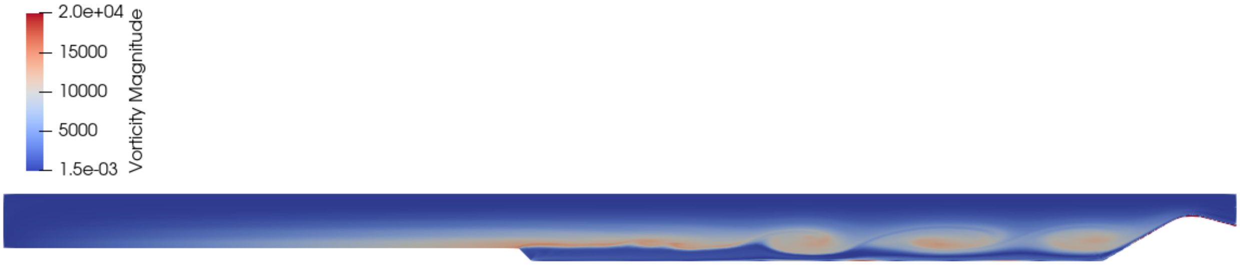

Figure 9: Vortex shedding phenomena appearance in the chamber

First, the fixed mass flow rate simulation was used to verify the appearance of the vortex shedding, the frequency of the instability and the quality of the mesh. Figure 9 shows the vorticity field in the motor. The vortexes due to the propellant grain steps are visible. The pressure signal is taken at the front end of the motor and analysed to check the frequency and amplitude of this instability. Figure 10a shows the pressure signal stabilisation around the mean chamber pressure and the presence of regular oscillations. The amplitude of the signal is computed throughout the stabilisation showing the relatively low level of instability in the chamber. A Fourier transform is done on the signal and shows in figure 10b the different frequencies exited by the vortex shedding phenomena.

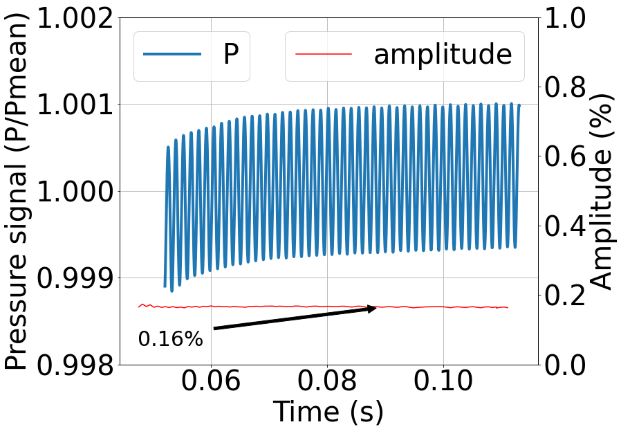

(a) Pressure signal at the front end of the C1x motor

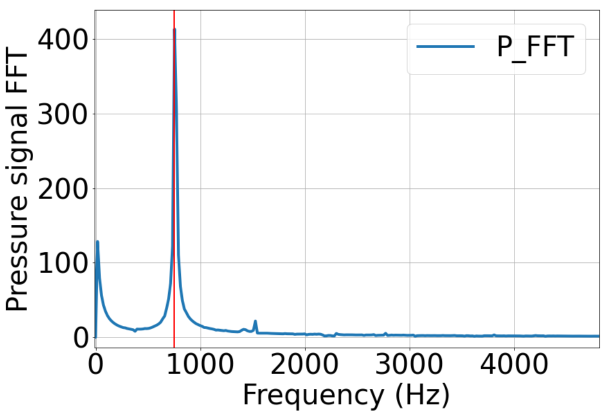

(b) Fourier transform of the pressure signal at the front end of the motor

Figure 10: Fixed mass flow rate at the burning surface simulation

The exited frequency in the chamber is around $760Hz \pm 10Hz$ for a $50ms$ signal analysis, which corresponds approximatively to the first longitudinal acoustic mode of the chamber. The signal is clear, and there are no harmonics. It is then interesting to compare the effect of a Saint Robert and Vieille law on the instability level and frequency. The second simulation was done with a propellant boundary condition taking a pyrolysis law corresponding to the same mass flow rate for the chamber pressure. Figure 11a shows the pressure signal over time and the amplitude of the oscillations observed at the motor's front end.

The response function of the propellant with a Saint Robert and Vieille law is theoretically equal to the pressure exponent of the law. Therefore, this study aims to estimate the intensity of the propellant response and compare it with the fixed mass flow rate one. There is no phase difference between the mass flow rate signal and the pressure signal as for the fixed mass flow rate simulation. However, the amplitude of the pressure oscillation observed is bigger and the response function computation gives exactly the Saint Robert and Vieille law pressure exponent value, that is 0.48. The frequency has also been verified and checked to be equal to the first acoustic mode of the motor. The appearance of

DOI: 10.13009/EUCASS2022-4583

other frequencies has also been checked in figure11b with a Fourier transform of the signal on a $50ms$ sample analysis. The appearance of a harmonic at $18200Hz$ which corresponds to the first radial acoustic mode of the chamber has been observed. The main frequency is still at $760Hz \pm 10Hz$ but the flow in the chamber is more perturbed with this model.

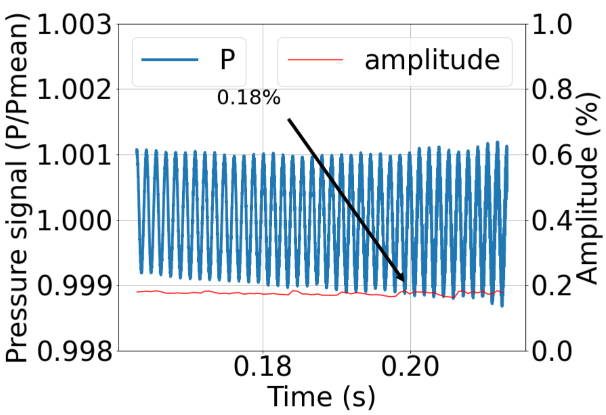

(a) Pressure signal at the front end of the C1x motor

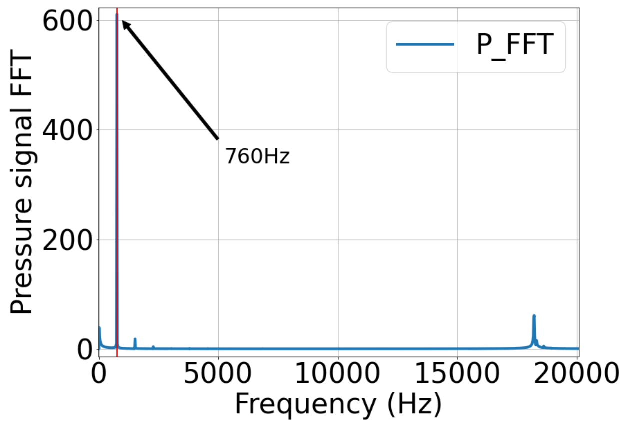

(b) Fourier transform of the pressure signal at the front end of the motor

Figure 11: Saint Robert and Vieille pyrolysis law burning surface simulation

The last part of the simulation on the c1x motor was using the KTZ model. The response parameter used here is the one used by Kuentzmann in [1] except for the Saint Robert and Vieille law that is the same as the preceding. The natural instability observed in the previous simulations show that the pressure oscillation amplitude is relatively low. Therefore, the response expected using the KTZ model is the linear response. The pressure signals are analysed to verify this response function.

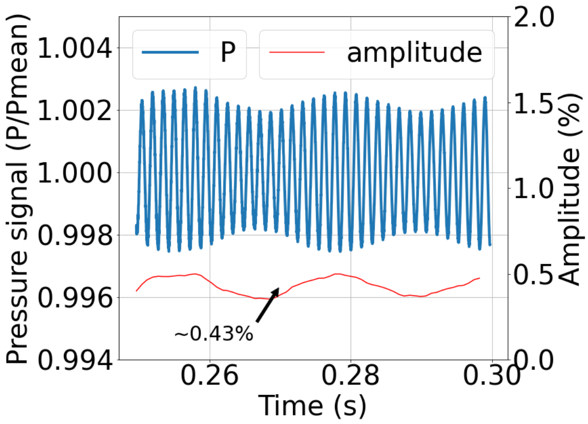

(a) Pressure signal at the front end of the C1x motor

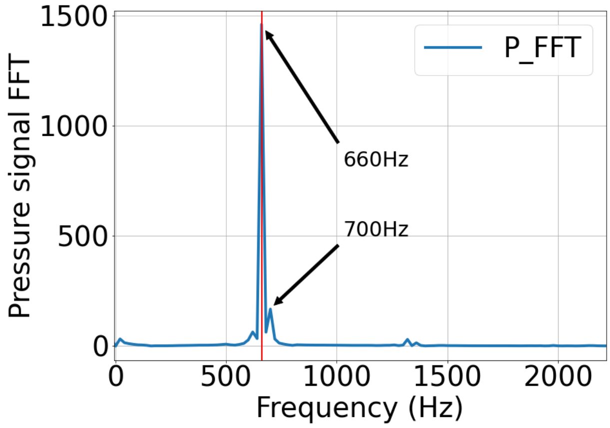

(b) Fourier transform of the pressure signal at the front end of the motor

Figure 12: KTZ model at the burning surface simulation

The pressure signal at the front end on figure 12a shows a bigger pressure oscillation amplitude. However, the frequencies observed in the simulation are quite different from the previous simulations. The Fourier transform of the signal has been computed on a $50ms$ sample. In fact, there are three frequency peaks visible in figure 12b at $660Hz \pm 25Hz$, $700Hz \pm 23Hz$ and $620Hz \pm 18Hz$. The first two are more significant than the third one and explain the the form of the pressure signal obtained. Some higher harmonics are also visible at the first radial mode but at lower amplitude compared to the main one. The analysis is done by approximating the signal by a perfect monochromatic sinusoid and the computation of the response function is done by estimating the phase difference between the mass flow rate and pressure signals at the burning surface and their amplitude. Figure 13a shows these signals. The results are summarized in table 2 and show that the imaginary part is negative.

DOI: 10.13009/EUCASS2022-4583

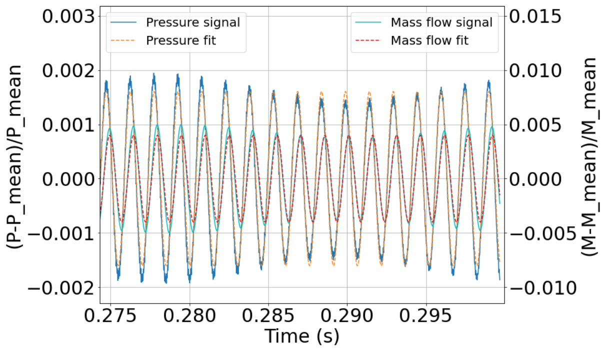

(a) Mass flow rate and pressure signal fitting for the KTZ model simulation

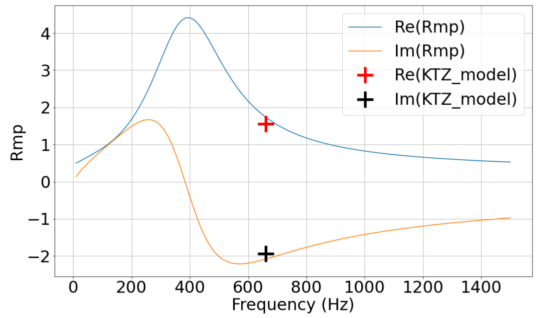

(b) Linear theoretical response function and model position

Figure 13: Response computation for KTZ model boundary condition

Model	Frequencies	Amplitude (%)	Re(Rmp)	Im(Rmp)
Fixed	$760Hz$	0.16%	0	0
APn	$760Hz$ ($18200Hz$)	0.18%	0.48	0
KTZ	$660Hz$ ($620Hz$, $700Hz$, $18200Hz$)	0.43%	1.56	-1.94

Table 2: Response function computation results for the C1x simulation

The theoretical linear response function can be computed and is plotted on figure 13b. The model response point is shown and it's slightly under the prevision the linear theorem. It can be explained by the monochromatic approximation of the signals that doesn't take into account the contribution on the response of secondary frequencies. The acoustic first mode of the c1x motor is above the peak frequency of the response model used in the simulation nevertheless the importance of the response effect on the instability in the chamber is demonstrated. The oscillation generated by the vortex shedding are amplified and dispersed by the propellant response and thus the characterisation of the propellant to pressure oscillation is of mean importance in order to take into account this effect on motor early simulations.

6. Modulated exhaust jet burner

The propellant response function can be characterized thanks to an experimental setup. Through the years, several setups have been developed for this purpose. At ONERA, the modulated exhaust jet thruster (MEJT) was developed by Barrère and improved by Kuentzmann [24, 25]. Figure 14a is the scheme of this setup.

A rotating wheel generates pressure oscillations at the nozzle's throat. The combustion chamber is designed to be small enough to avoid wave propagations and ensure the pressure oscillations move uniformly in the volume. The wheel rotating speed is fixing the frequency of the pressure oscillations generated. The amplitude of the oscillations is defined by the distance between the wheel centre and the exit throat centre. If this distance is large enough, the wheel teeth will not cover a large part of the exit surface, so that the oscillation amplitude will be low. In the same way, if this distance is small, then the teeth of the wheel will cover more surface of the exit surface, and thus, the amplitude will be significant. In order to avoid exciting acoustics mode of the chamber, the achiveable frequency is around 1kHz defined as the first acoustic mode of the thruster. Another advantage of the small combustion chamber is that the pressure sensor placed at the periphery of the chamber will give a pressure signal similar to the one obtained at the burning surface with a small deviation. The availability of the KTZ response model as a boundary condition of the CFD code CEDRE allows us to do some numerical simulation on the set-up geometry to reproduce the experiments and thus characterise the model parameter necessary to describe the propellant response [26].

The numerical simulation was done using a 2D axi-symmetric simulation on the MEJT geometry. Figure 14b shows the geometry used in the simulation with the position of the sensors. Verifying the deviation between the "physi-

DOI: 10.13009/EUCASS2022-4583

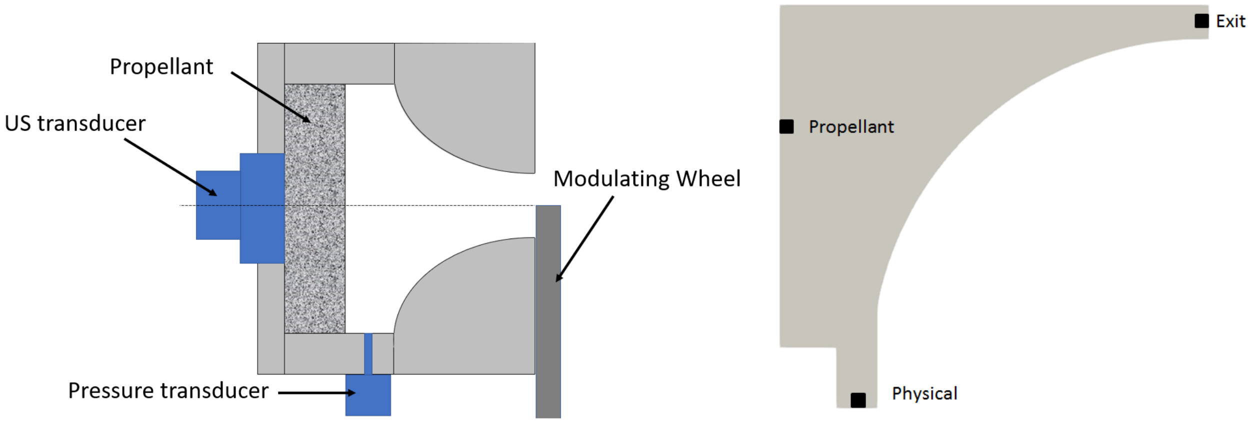

(a) Modulated exhaust jet burner (b) 2D axisymmetric geometry

Figure 14: MEJT scheme and geometrical representation for numerical simulation

cal" and "propellant" sensors was first done. The chamber being small the deviation observed appeared to be negligible. Then the mass flow rate and the pressure signal were directly taken from the "propellant" sensor. The objective of this study was to reproduce the effect of the rotating wheel on the burning propellant. For the propellant surface representation three boundary conditions were tested, fixed mass flow rate, Saint Robert and Vieille law and the KTZ model.

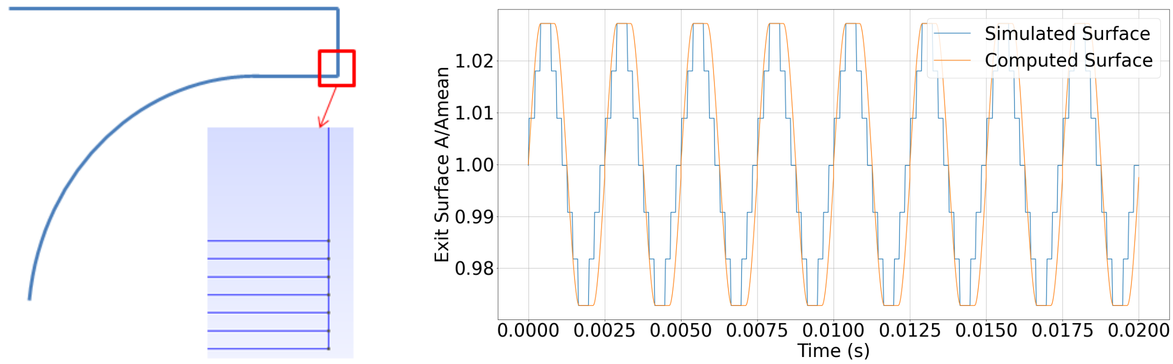

(a) Cutted exit surface (b) Exit surface evolution

Figure 15: Simulation of the rotating wheel effect of the Exit surface simulation

The tricky part in this simulation is reproducing the effect of the rotating wheel on the pressure signal observed in the combustion chamber. In 2D axisymmetric, this effect was simulated by assuming that the exit throat was shrunk and widened periodically at the wheel frequency. To do so, the exit surface was cut into several small surfaces (as shown in figure 15a) that were closed step by step, respecting the wanted frequency. Figure 15b shows the approximation of the actual exit surface modulation throughout time done with this method for a 400Hz and less than 1% of the mean pressure amplitude oscillations.

For each propellant simulation method, the Fourier transform of the pressure signal, the propellant's pressure coupled response, and three frequencies, 400Hz, 600Hz and 800Hz, were studied. First, a steady-state simulation was established, and then each frequency was simulated with a simulation recovery of the steady-state result. The stabilisation of the instability was reached, and the signal was analysed.

The Fourier transform of the MEJT simulation with the KTZ model shows that the frequencies wanted are aimed. Figure 16 shows the three Fourier transform of the different frequencies exited. The signal obtain is clearly showing that even if there are some small harmonics the main frequency exited is the wanted one. Figure 17 shows the evo-

DOI: 10.13009/EUCASS2022-4583

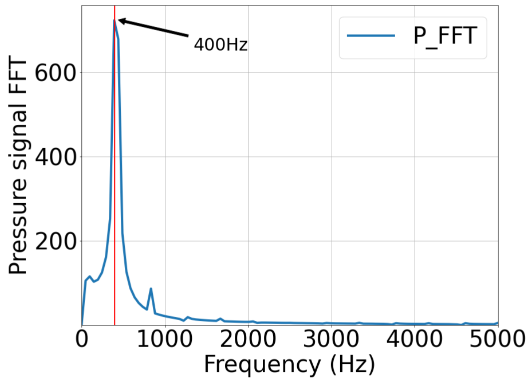

(a) 400 Hz

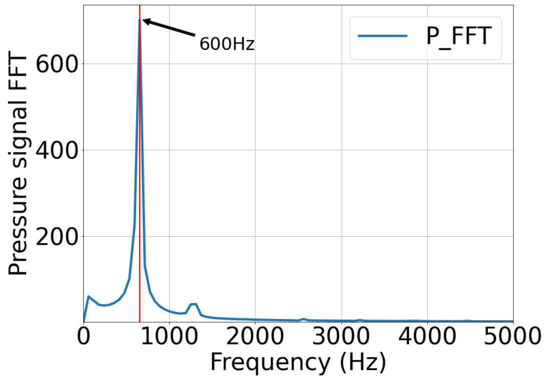

(b) 600 Hz

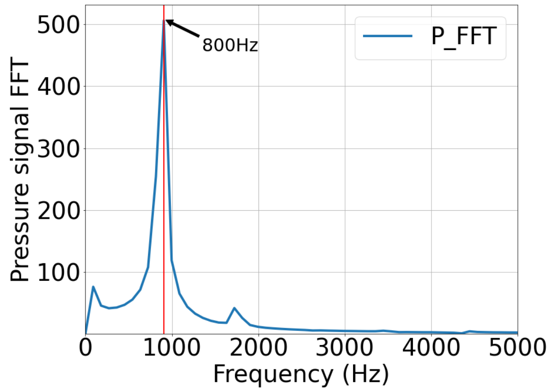

(c) 800 Hz

Figure 16: Fourier transform of the pressure signals with the KTZ model

lution of the pressure signal amplitude throughout the computation and the final amplitude reached by the different simulations for a 400Hz rotating wheel. These figures are showing the presence of small amplitude perturbations that explain the other frequency peak observed in the Fourier transform.The signals are well established at the end of the simulation, and several periods are available for response computation and can be treated as perfect sinusoid at the wanted frequency.

For the fixed mass flow rate simulation, it is clear that there is no response of the propellant. The mass flow is fixed, and the equation (1) is zero, but the simulation gives a reference for comparison with the two other models. The Apn burning law and KTZ model signals were approximated with a perfect sinusoid to catch the amplitude and the phase difference between the signals. Figure 18 shows, (a) the phase difference between the mass flow rate and the pressure signals and (b) the fitting of these signals with the sinusoid for the 400Hz simulation using the KTZ model for the propellant.

Thanks to these approximations, the response function of each frequency has been computed. Figure 19a shows the response function obtained for the Apn burning law. We can observe that there is no phase difference between the mass flow rate and the pressure signal and that the gain obtained between the two curves is equal to the pressure exponent used in the burning law. This result is coherent with the theory. Figure 19b shows the response function obtained for the KTZ model.

The response curve seems to be shifted compared to one observed in the validation of the model. This can be explained by the burning law used in the model that was not the same but was the one observed in the experimental set-up. The easy way to prove that the response peak of this propellant is shifted compared to the one studied in the validation part, is to compute the theoretical peak of a linear response (15). This peak response point can be computed by seeking the frequency at which the imaginary part of the response function (1) is equal to zero. The expression of the reduced frequency at the peak is therefore (15).

DOI: 10.13009/EUCASS2022-4583

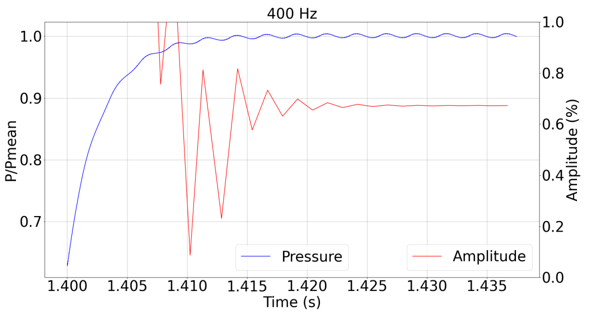

(a) Fixed mass flow rate

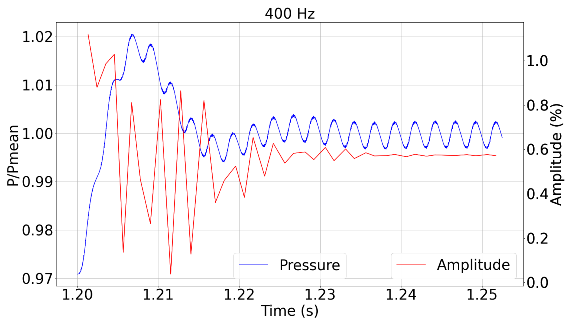

(b) Saint Robert and Vieille law

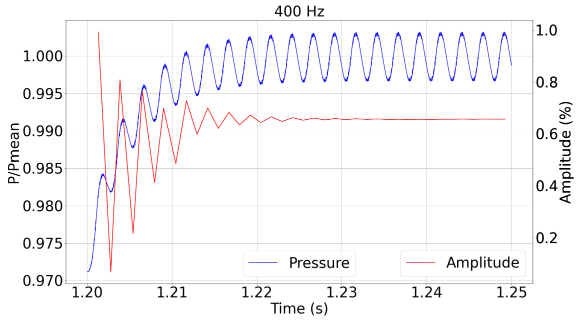

(c) KTZ model

Figure 17: Simulation of the MEJT with (a) Fixed mass flow rate, (b) Apn burning law, (c) KTZ model at 400Hz.

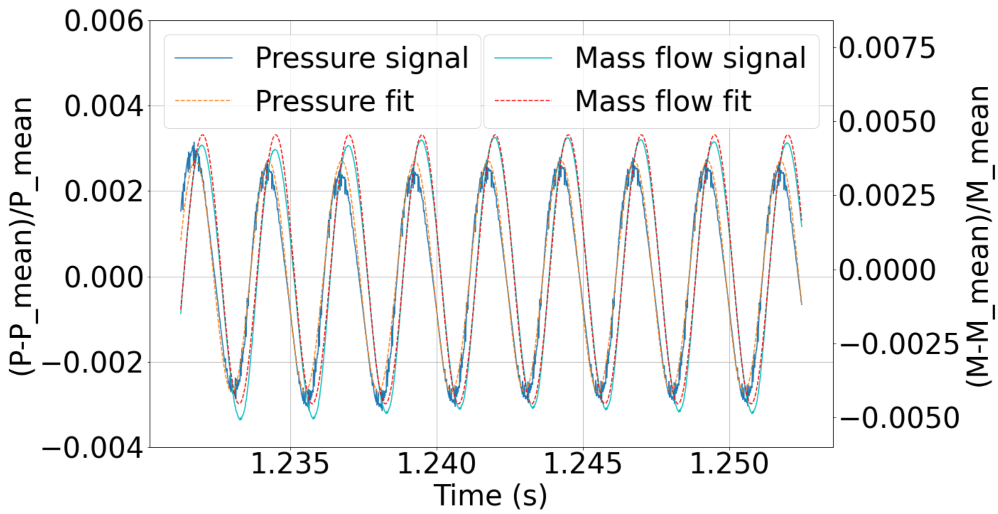

Figure 18: Mass flow rate and Pressure signal approximation with a perfect sinusoid for the 400Hz simulation using KTZ model

$$\Omega = \sqrt{A\left(A + \frac{1}{2} - \frac{\sqrt{8A+1}}{2}\right)} \tag{15}$$

In our case, with the combustion law used with this propellant, the A was equal to 12.13 and so the peak frequency is estimated at $202.8Hz$. A simulation of the MEJT at 200Hz has been done to verify the presence of the peak. The computation of the response shows that we obtain a bigger response of the propellant which allows use to complete 19b

DOI: 10.13009/EUCASS2022-4583

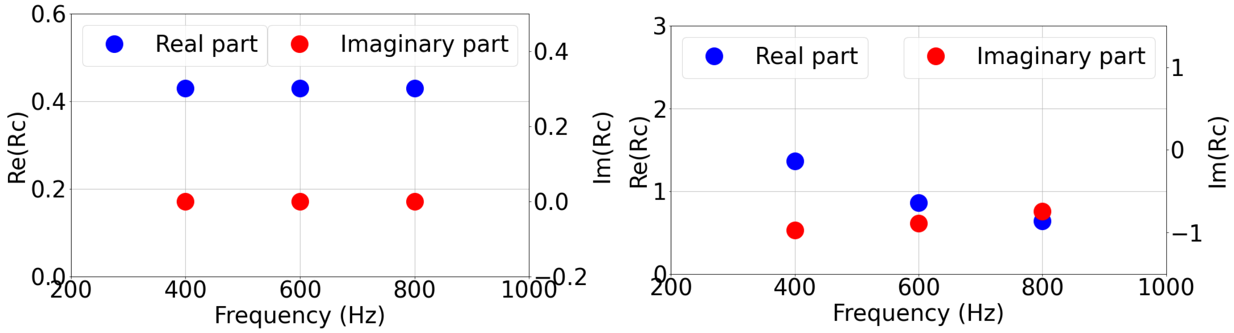

(a) Apn burning law

(b) KTZ model

Figure 19: Response function computed for the two burning models for three frequencies

with a new point on figure 20. The value of teh theoretical peak frequency appeared to be lower than the one observed experimentally. This result shows that the response aprametrs arre not adapted to a realistic propellant.

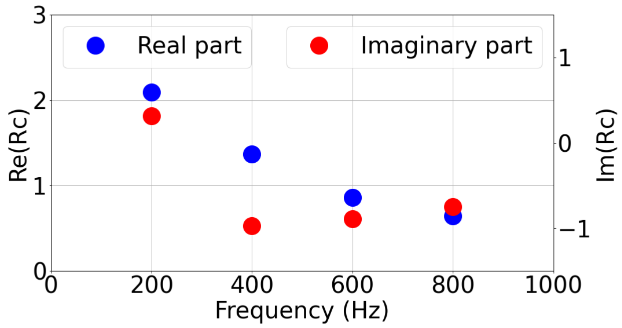

Figure 20: Response function completed with the KTZ model

These results show this set-up's purpose to characterise the solid propellant's response and how the model can predict its behaviour. In [26], the experimental campaign has been explained and analysed. In the first place, linear oscillations characterise the model parameters necessary to reproduce the experiments numerically. Then the model could be used to simulate the response of solid propellant to the greater amplitude of oscillations. Moreover, the numerical simulation of the set-up allows for to study of the different hypotheses done in the post-processing of the experimental data that will be done in future work.

7. Conclusion

A solid propellant's pressure-coupled response function must be characterised and well represented in preliminary studies. Therefore, some models must be constructed to consider the response effect on internal instabilities. The KTZ model integrated into the CFD code CEDRE represents what is happening in the linear theoretical domain and proved to be used up to greater instability amplitudes.
The TEP motor study has shown the importance of considering the response function on the level of instability found in the combustion chamber. Moreover, a comparison of the KTZ model and theoretical models previously studied by an acoustic balance has been made. The interest of the model to compute the global damping of a combustion chamber has been demonstrated. The motor being stable, stabilising the pressure signal was ensured, but it could not be the case for unstable motors.
The C1x motor is naturally unstable, with a vortex shedding phenomenon appearing in the combustion chamber. The application of the KTZ model on this test case has proved the importance in taking into account the response phenomena in order to anticipate the level of pressure oscillation in a chamber. The comparison with other propellant modelling have shown thet the KTZ model is able of describing this effect as soon as the propellant is well characterized.

Finally, experimental means are the best way to characterise a solid propellant's response function. Therefore, the numerical study of the MEJT has shown interest in reproducing experimental conditions in a 2D axisymmetric

DOI: 10.13009/EUCASS2022-4583

simulation that is cheaper and representative of the experiment. The phase difference between the mass flow rate and the pressure signal has been shown for a fixed response model parameter. The interest in putting some numerical sensors on the propellant has been proven. However, it is still essential to use the MEJT experiment to characterise real propellants and then define our model parameter in order to be able to simulate greater pressure oscillation amplitudes. The next step of this study will be both numerical and experimental to define the response of a real solid propellant and to observe the effect of great amplitude of the instabilities in the chamber. A comparison between the non-linear test campaign and the numerical result would be of great interest to verify the capabilities of the KTZ model.

8. Acknowledgements

The present work was conducted thanks to a Ph.D grant co-funded by Centre National d'Etudes Spatiales, CNES (J. Pichillou, Technical Advisor) and ONERA.

References

[1] P. Kuentzmann. Modèles de combustion instationnaire des propergols solides composites. *La Recherche Aérospatiale*, pages 77–93, 1978.

[2] B. V. Novozhilov. Burning of a powder under harmonically varying pressure. *Journal of Applied Mechanics and Technical Physics*, 6(6):103–106, November 1965.

[3] B. V. Novozhilov. Theory of nonsteady burning and combustion stability of solid propellants by the Zeldovich-Novozhilov method. In *Nonsteady Burning and Combustion Stability of Solid Propellants*, pages 601–641. American Institute of Aeronautics and Astronautics, 1990.

[4] R. W. Hart and F. T. McClure. Combustion instability: acoustic interaction with a burning propellant surface. *The Journal of Chemical Physics*, 30(6):1501–1514, June 1959.

[5] M. R. Denison and Eric Baum. A simplified model of unstable burning in solid propellants. *ARS Journal*, 31(8):1112–1122, August 1961.

[6] F. Culick. A review of calculations for unsteady burning of solid propellant. *AIAA Journal*, 6, December 1968.

[7] James S T'ien. Oscillatory burning of solid propellants including gas phase time lag. *Combustion Science and Technology*, 5(1):47–54, March 1972.

[8] I.-TE Huang and M. M. Micci. Unsteady gas phase analysis of homogeneous solid propellant combustion. *Combustion Science and Technology*, 75(1-3):73–88, January 1991.

[9] Paul Clavin and David Lazimi. Theoretical analysis of oscillatory burning of homogeneous solid propellant including non-steady gas phase effects. *Combustion Science and Technology*, 83(1-3):1–32, May 1992.

[10] F. Culick and G. Isella. Modeling the combustion response function with surface and gas phase dynamics. In *38th Aerospace Sciences Meeting and Exhibit*. American Institute of Aeronautics and Astronautics, 2000.

[11] William Nachbar. A theoretical study of the burning of a solid propellant sandwich. In *Solid propellant rocket research*, pages 207–226. New York, 1960.

[12] Martin Summerfield, editor. *Solid propellant rocket research*. American Institute of Aeronautics and Astronautics, New York, January 1960.

[13] M. W. Beckstead, R. L. Derr, and C. F. Price. A model of composite solid-propellant combustion based on multiple flames. *AIAA Journal*, 8(12):2200–2207, December 1970.

[14] B. Rasmussen and R. A. Frederick. Nonlinear heterogeneous model of composite solid-propellant combustion. *Journal of Propulsion and Power*, 18(5):1086–1092, September 2002.

[15] J. N. Levine and F. E. C. Culick. Nonlinear analysis of solid rocket combustion instability. Volume II. Technical report, ULTRASYSTEMS INC IRVINE CALIF, August 1974.

[16] F. Culick. T-Burner testing of metallized solid propellants. page 274, October 1974.

DOI: 10.13009/EUCASS2022-4583

[17] L. Strand. Laboratory test methods for combustion-stability properties of solid propellants. In *Nonsteady Burning and Combustion Stability of Solid Propellants*, pages 689–718. American Institute of Aeronautics and Astronautics, 1990.

[18] F. Cauty. Solid-propellant combustion response function from direct measurement methods: ONERA experience. *Journal of Propulsion and Power*, 15(6):837–843, 1999.

[19] J. C. Traineau and P. Kuentzmann. Some measurements of solid propellant burning rates in nozzleless motors. In *20th Joint Propulsion Conference*. American Institute of Aeronautics and Astronautics, 1984.

[20] Z. Wang, P. Liu, and W. Ao. A reduced-order model of thermoacoustic instability in solid rocket motors. *Aerospace Science and Technology*, 97:105615, February 2020.

[21] Francois Vuillot, Thierry Basset, Joel Dupays, Eric Daniel, and Nicolas Lupoglazoff. 2D Navier-Stokes stability computations for solid rocket motors - Rotational, combustion and two-phase flow effects. In *33rd Joint Propulsion Conference and Exhibit*, Seattle,WA,U.S.A., July 1997. American Institute of Aeronautics and Astronautics.

[22] J. Dupays, M. Prevost, P. Tarrin, and F. Vuillot. Effects of particulate phase on vortex shedding driven oscillations in solid rocket motors. In *32nd Joint Propulsion Conference and Exhibit*, Lake Buena Vista,FL,U.S.A., July 1996. American Institute of Aeronautics and Astronautics.

[23] Nicolas Lupoglazoff and Francois Vuillot. Comparison between firing tests and numerical simulation of vortex shedding in 2-d test solid motor. 07 1993.

[24] M. Barrère and L. Nadaud. Prevision of Unstable Operation Domains of Solid Propellant Rocket Motors. In L. G. Napolitano, P. Contensou, and W. F. Hilton, editors, *Astronautical Research 1971*, pages 265–284, Dordrecht, 1973. Springer Netherlands.

[25] P. Kuentzmann and L. Nadaud. Réponse des propergols solides aux oscillations de pression et de vitesse. *Combustion Science and Technology*, 11(3-4):119–139, September 1975. Publisher: Taylor & Francis.

[26] M. Carricart. Solid propellant response function estimation with a modulated exhaust jet apparatus and simulation. In *8th Space-Propulsion conference*. 3af, Association Aéronautique at Astronautique de France, May 2022.